Thermodynamic glass transition in a spin glass without time-reversal symmetry

Raquel Alvarez Baños[a,b], Andres Cruz[a,b], Luis Antonio Fernandez[a,c], Jose Miguel Gil-Narvion[a], Antonio Gordillo-Guerrero[a,d], Marco Guidetti[a], David Iñiguez[a,e], Andrea Maiorano[a,f], Enzo Marinari[f], Victor Martin-Mayor[a,c], Jorge Monforte-Garcia[a,b], Antonio Muñoz Sudupe[c], Denis Navarro[g], Giorgio Parisi[f,1], Sergio Perez-Gaviro[a], Juan Jesus Ruiz-Lorenzo[a,h], Sebastiano Fabio Schifano[i], Beatriz Seoane[a,c], Alfonso Tarancon[a,b], Pedro Tellez[b], Raffaele Tripiccione[i], and David Yllanes[a,c]

[a]Instituto de Biocomputación y Física de Sistemas Complejos (BIFI), 50009 Zaragoza, Spain; [b]Departamento de Física Teórica, Universidad de Zaragoza, 50009 Zaragoza, Spain; [c]Departamento de Física Teórica I, Universidad Complutense, 28040 Madrid, Spain; [d]Departamento de Ingeniería Eléctrica, Electrónica y Automática, Universidad de Extremadura, 10071 Cáceres, Spain; [e]Fundación Agencia Aragonesa para la Investigación y el Desarrollo (ARAID), Diputación General de Aragón, 50009 Zaragoza, Spain; [f]Dipartimento di Fisica, Università di Roma "La Sapienza", Istituto dei Processi Chimici Fisici-Consiglio Nazionale delle Ricerche (IPCF-CNR) and Istituto Nazionale Fisica Nucleare (INFN), 00185 Roma, Italy; [g]Departamento de Ingeniería, Electrónica y Comunicaciones and I3A, Universidad de Zaragoza, 50018 Zaragoza, Spain; [h]Departamento de Física, Universidad de Extremadura, 06071 Badajoz, Spain; and [i]Dipartimento di Fisica, Università di Ferrara and Istituto Nazionale Fisica Nucleare (INFN)—Sezione di Ferrara, 44122 Ferrara, Italy

Contributed by Giorgio Parisi, February 29, 2012 (sent for review January 17, 2012)

Spin glasses are a longstanding model for the sluggish dynamics that appear at the glass transition. However, spin glasses differ from structural glasses in a crucial feature: they enjoy a time reversal symmetry. This symmetry can be broken by applying an external magnetic field, but embarrassingly little is known about the critical behavior of a spin glass in a field. In this context, the space dimension is crucial. Simulations are easier to interpret in a large number of dimensions, but one must work below the upper critical dimension (i.e., in *d* < 6) in order for results to have relevance for experiments. Here we show conclusive evidence for the presence of a phase transition in a four-dimensional spin glass in a field. Two ingredients were crucial for this achievement: massive numerical simulations were carried out on the Janus special-purpose computer, and a new and powerful finite-size scaling method.

de Almeida-Thouless line | critical exponents | parallel tempering | scaling corrections

The glass transition differs from standard phase transitions in that the equilibration time of glass formers (supercooled liquids, polymers, proteins, superconductors, etc.) diverges without dramatic changes in their structural properties (1–3). The reconciliation of the dynamic slowdown with the apparent immutability of glass formers is a major challenge for condensed matter physics.

Spin glasses [which are disordered magnetic alloys (4)] enjoy a privileged status in this context, as they provide the simplest model system both for theoretical and experimental studies of a glassy dynamics. On the experimental side, time-dependent magnetic fields provide a wonderful tool to probe the dynamic response, which can be accurately measured with a SQUID (for instance, see ref. 5). On the theoretical side, magnetic systems are notably easier to model and to simulate numerically. In fact, special-purpose computers have been built for the simulation of spin glasses (6–9).

Yet, spin glasses differ from most glassy systems in a crucial feature: like all magnetic systems, they enjoy time-reversal symmetry in the absence of an applied magnetic field. In fact, we now know that their glassy dynamics are due to a bona fide phase transition in which the time-reversal symmetry is spontaneously broken (10–12). Yet, in the presence of an applied magnetic field, the experimental spin-glass dynamics is just as glassy, although the field explicitly breaks the symmetry.

However, whether spin glasses in a magnetic field undergo a phase transition has been a long-debated and still open question (see refs. 13, 14 for recent, opposed views). In the mean-field approximation, which is valid for large spatial dimension down to the upper critical dimension $d_\mathrm{u} = 6$ (15), the de Almeida-Thouless line separates the high-temperature paramagnetic phase from the glassy phase (16)*. Yet, recent numerical simulations in spatial dimensions below d_u did not find the transition in a field (18, 19). Experimental studies have been conducted as well, with conflicting conclusions (20–23). In spite of these difficulties, it has been argued that the would-be spin-glass transition in a magnetic field sets the universality class for the thermodynamic glass transition (24).

Here, we present conclusive evidence for a spin-glass transition in the presence of an external magnetic field in the four-dimensional Edwards-Anderson model (hence, well below d_u). This result was obtained by means of a large-scale numerical simulation, partly carried out on the Janus computer (8). Due to some pathologies of the spin-glass correlation function (25), our analysis method departs from the standard one. We compute critical exponents, widely differing from the zero field case, with an accuracy of 5%. The failure of previous work to identify the transition is explained in terms of very strong corrections to scaling.

Results

We consider the Edwards-Anderson model with Ising spins ($S_\mathbf{x} = \pm 1$) sitting on the nodes of a $D = 4$ cubic lattice of size $V = L^D$. Our Hamiltonian is

$$\mathscr{H} = -\sum_{\langle \mathbf{x},\mathbf{y}\rangle} J_{\mathbf{xy}} S_\mathbf{x} S_\mathbf{y} - h \sum_\mathbf{x} S_\mathbf{x}, \qquad [1]$$

where $\langle \mathbf{x}, \mathbf{y}\rangle$ indicates that the sum is taken over all nearest-neighbor pairs and each $J_\mathbf{xy}$ is ± 1 with 50% probability.

As stated in the introduction, we want to investigate whether this system experiences a second-order phase transition in the presence of a nonzero magnetic field h. The presence of such a continuous transition is typically checked through the study of some correlation length ξ, which is a good marker of scale invariance.

To this end, we begin by defining the spatial autocorrelation function $G(\boldsymbol{r})$. This definition can actually be done in several ways

---

Author contributions: V.M.-M., G.P., J.J.R.-L., and A.T. designed research; R.A.B. and L.A.F. performed research; J.M.G.-N., A.M., D.N., S.F.S, P.T., and R.T. contributed Janus hardware/software; R.A.B., L.A.F., A.C.,J., M.G.-N., A.G.-G., M.G., D.I., E.M., V.M.-M., J.M.-G., A.M.S., G.P., S.P.-G., J.J.R.-L., B.S., A.T., and D.Y. analyzed data; R.A.B., L.A.F., V.M.-M., D.N., and D.Y., wrote simulation and analysis codes; and V.M.-M. and D.Y. wrote the paper.

The authors declare no conflict of interest.

*A more careful analysis is needed in order to reach the same conclusion in the range $6 < d < 8$ (17).

[1]To whom correspondence should be addressed. E-mail: giorgio.parisi@roma1.infn.it.

This article contains supporting information online at www.pnas.org/lookup/suppl/doi:10.1073/pnas.1203295109/-/DCSupplemental.

in the presence of a magnetic field (see *Materials and Methods* for details). Then, ξ is just the characteristic length for the long-distance decay of $G(\boldsymbol{r})$. In order to arrive at an appropriate definition for finite lattice systems, one typically considers the propagator in Fourier space, $\hat{G}(\boldsymbol{k})$, and defines the second-moment correlation length ξ_2 from a truncated Ornstein-Zernike expansion -Eqs. **11** and **12**.

We have plotted ξ_2 in Fig. 1 for all our lattice sizes and $h = 0.3$. There is a clear change of regime from the high-temperature behavior, where we can see a finite enveloping curve, to the growth of the correlation length at low temperatures. We intend to show that this change of regime actually corresponds to a phase transition, using finite-size scaling (26).

In principle, at the transition point there should be scale invariance in the system, meaning that

$$\xi_2/L = f_\xi(L^{1/\nu}t) + \ldots, \qquad t = \frac{T - T_c(h)}{T_c(h)}, \qquad [2]$$

where ν is the thermal critical exponent and the dots represent corrections to leading scaling, expected to be unimportant for large lattice sizes. Therefore, the curves of ξ_2/L for large lattices should intersect at the critical point $t = 0$. Previous attempts to find T_c using this approach, however, have generally concluded that these intersections cannot be found (or, rather, that the apparent intersection point goes to $T = 0$ as L grows) (18, 19). Indeed, if we look at the top box of Fig. 2, we see that either there is no phase transition or ξ_2 is completely in a preasymptotic regime.

Some authors, working with $D = 1$ models with long-range interactions, have already offered an explanation for this apparent lack of scale invariance: the propagator behaves anomalously, but only for the $\boldsymbol{k} = 0$ mode (25). This irregular behavior results in very strong corrections to the leading scaling term of Eq. **2**, because the second-moment correlation length depends on $\hat{G}(\boldsymbol{k} = 0)$. We have checked numerically that this phenomenon is also at play in our $D = 4$ system, which is probably a general consequence of the presence of Goldstone bosons in the system (see *Materials and Methods* for a discussion of this phenomenon).

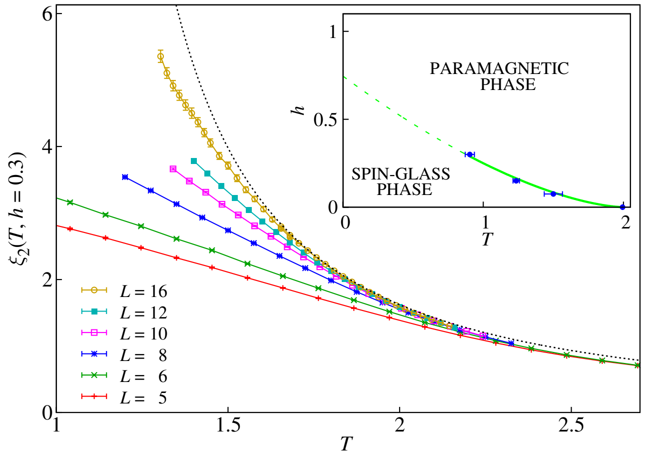

Fig. 1. Plot of the second moment correlation length ξ_2 -Eq. **12**- against temperature in an external field $h = 0.3$. There is a clear crossover from the convergence to a finite envelope at high T to the more rapid growth at low T. As this paper shows, this crossover is caused by the onset of a spin-glass transition. The dotted black line is a fit to a critical divergence as $\xi_2^\infty \propto [T - T_c(h)]^{-\nu}$, where T_c and ν are taken from Table 1. The inset is a sketch of the phase diagram (the de Almeida-Thouless line), including a fit to the Fisher-Sompolinsky scaling $h_c^2(T) \simeq A|T - T_c^{(0)}|^{\beta^{(0)}+\gamma^{(0)}}$ (17). The quantities with a superindex (0) are the values for the $h = 0$ critical point (33, 34), so the only free parameter is the amplitude A. In this and all other figures the error bars represent one standard deviation.

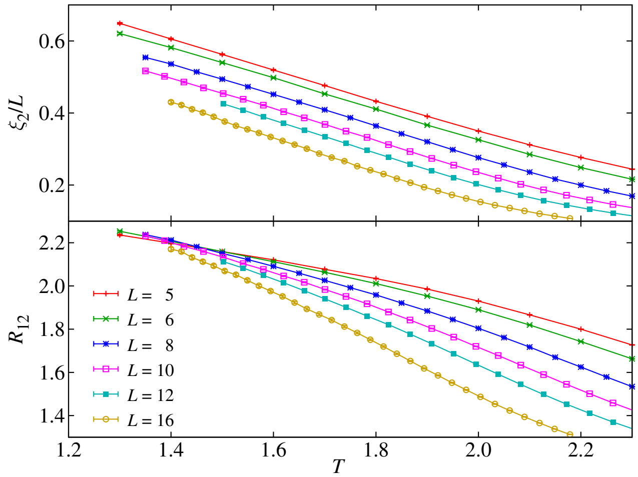

Fig. 2. Top: plot of ξ_2/L as a function of temperature for all our lattice sizes at $h = 0.15$. According to leading-order finite-size scaling, the curves for different sizes should intersect at the phase transition point, but this behavior is not seen in the plot. This apparent lack of scale invariance has led some authors to conclude that there is no phase transition in this system. Bottom: Same plot of the dimensionless ratio R_{12}, Eq. **3**, which should have the same leading-order scaling as ξ_2/L. Unlike the correlation length, however, R_{12} does exhibit very clear intersections, signalling the presence of a second-order phase transition. The dramatic improvement in the scaling, compared to the top box, is explained by the pernicious effect on ξ_2 of the anomalous behavior in the correlation function for zero momentum.

In order to avoid this issue, in this paper we take a different approach, eschewing ξ_2/L in favor of a new dimensionless ratio as the basic quantity for our finite-size scaling study. In particular, we shall consider ratios of higher momenta:

$$R_{12} = \frac{\hat{G}(\boldsymbol{k}_1)}{\hat{G}(\boldsymbol{k}_2)}, \qquad [3]$$

where $\boldsymbol{k}_1 = (2\pi/L, 0, 0, 0)$, $\boldsymbol{k}_2 = (2\pi/L, 2\pi/L, 0, 0)$ (and permutations) are the smallest nonzero momenta compatible with the periodic boundary conditions. Notice that, while our use of R_{12} as a basic parameter is not standard, this is not in any way a strange quantity. In fact, it is a universal renormalization-group invariant, whose value in the large-L limit for a paramagnetic system should be $R_{12}(T > T_c) = 1$. At the critical point, however, $R_{12}(T_c) > 1$. For instance, using conformal theory relations (27, 28), we have computed the critical ratio exactly for the nondisordered $D = 2$ Ising model: $R_{12}^{\text{Ising}}(T_c) = 1.694024\ldots$.

To leading order, R_{12} should have the same scaling behavior as ξ_2/L, namely,

$$R_{12} = f_{12}(L^{1/\nu}t) + [\text{scaling corrections}]. \qquad [4]$$

However, because this quantity avoids the anomalous $\boldsymbol{k} = 0$ mode, we expect that corrections to scaling be smaller. Indeed, in the bottom box of Fig. 2 we can see that the improvement in the scaling from the ξ_2 case is dramatic. Even though corrections to scaling are noticeable, for large sizes the intersections of the curves seem to converge. Notice as well that the high values of R_{12} in the neighborhood of the intersection point are not only far from the paramagnetic limit of $R_{12} = 1$, but also above the bound $R_{12} \leq 2$ that would result from a smooth behavior of the propagator (see the discussion following Eq. **11**).

Therefore, it is our working hypothesis that there is a phase transition, but one that is affected by large corrections to scaling. To substantiate this statement and actually compute the critical parameters, we must begin by somehow controlling these corrections. This analysis is rather technical, but not critical to our discussion, so we leave it for the *SI Text*, where we study the behavior of ξ_2/L at fixed R_{12} as a function of L. To leading order, this function should be constant, so it has allowed us to isolate the effect of the scaling corrections, parameterised as an extra term in $L^{-\omega}$ in [**2**] and [**4**] (see Fig. S1), where

$$\omega = 1.43(37). \qquad [5]$$

Now that we have the scaling corrections exponent ω, we can go back to study R_{12}. The easiest way to compute the critical parameters (T_c, ν, etc.) from a renormalization-group invariant such as R_{12} is the quotients method (29). Unfortunately, in our case the corrections to scaling are strong, and for some lattice sizes we do not actually reach the intersection point. Let us, therefore, consider an alternative procedure (30).

We assume (and therefore will test) that all points of the de Almeida-Thouless line ($h > 0$) belong to the same universality class. We begin by considering Eq. **4** and explicitly write the corrections to scaling, recall that $t = (T - T_c(h))/T_c(h)$,

$$R_{12}(T, L, h) = f_{12}(tL^{1/\nu}) + A(h, tL^{1/\nu})L^{-\omega} + \ldots. \qquad [6]$$

Now we define $T_R^L(h)$ as

$$R_{12}(T_R^L(h), L, h) = R. \qquad [7]$$

Therefore, if R is in the scaling region, i.e., not too far from $f_{12}(0)$, then

$$T_R^L(h) \simeq T_c(h) + B_{R,h}L^{-1/\nu}[1 + C_{R,h}L^{-\omega}]. \qquad [8]$$

Using this formula, keeping ω fixed to the value of [**5**], we can, in principle, estimate the critical exponent ν and the critical temperature $T_c(h)$. However, for a single value of R we do not have enough degrees of freedom in the fit. Therefore, following ref. 31, we consider several values of R and two values of the field, $h = 0.15$ and $h = 0.30$ at the same time in a joint fit, where ν is shared by all datasets and $T_c(h)$ is shared by all the datasets with the same h (see ref. 32 for full details on this fitting procedure). This global fit is plotted in Fig. 3, while the fit parameters can be seen in Table 1. We also include the critical temperature for $h = 0.075$, extrapolated with the value of ν computed for $h = 0.15$ and $h = 0.3$[†]. We have thus been able to obtain a precise determination of $T_c(h)$ and of the critical exponent ν. It is important to mention that the value of ν which, as we have seen, is universal for $h > 0$, is very different from that of the $h = 0$ case. As a consistency check of our nonstandard finite-size scaling method, we have run a smaller set of simulations for $h = 0$ and obtained $\nu^{(0)} = 0.96(11)$ and $T_c^{(0)} = 2.002(10)$, in good agreement with previous results for the $h = 0$ case (33, 34). We remark that both the critical temperature and $\nu^{(0)}$ widely differ from the values in Table 1.

The determination of the second independent critical exponent, the anomalous dimension η of the propagator, is much more difficult. In principle, we could consider the scaling of the propagator $\hat{G}(\boldsymbol{k})$ at fixed $R_{12} = R$. However, η is more affected by the scaling corrections than ν. In fact, as discussed in *SI Text*, we had to consider quadratic corrections to scaling, as $A_1L^{-\omega_{\mathrm{eff}}} + A_2L^{-2\omega_{\mathrm{eff}}}$, with $\omega_{\mathrm{eff}} = 2.2(3)$, in order to fit the data. Our final estimate is quoted in Table 1. Finally, we can combine our results in Table 1 to sketch the de Almeida-Thouless line, which is plotted in the inset to Fig. 1. We also show a very good fit to the Fisher-Sompolinsky scaling (17).

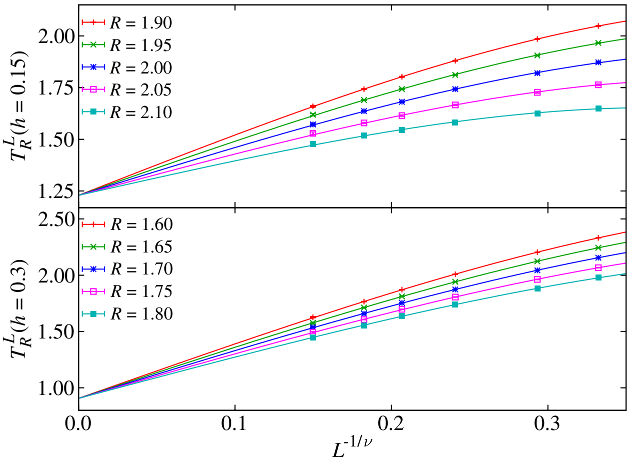

Fig. 3. Computation of the critical temperature $T_c(h)$ and the critical exponent ν. We compute the temperature $T_R^L(h)$ for which $R_{12}(T_R^L, L, h) = R$. For R inside the scaling region, these temperatures should approach the critical one according to [**8**]. We perform a joint fit for all the datasets in the plot, forcing all of them to share the same ν and forcing all sets with the same h to extrapolate to the same $T_c(h)$. The result of this fit, which had a chi-square per degree of freedom of $\chi^2/\mathrm{d.o.f.} = 40.2/37$ (P-value: 33%), can be seen in Table 1.

Let us finally mention that one may analyze our data as well under the assumption of the *absence* of the phase transition in a field. This analysis, which relies on refs. 35–37, is reported in *SI Text*. The data fail to follow basic scaling relations derived under the no-transition hypothesis (or, at least, they fail to scale within the range of system sizes that we could simulate, as can be seen in Fig. S2).

Discussion

In summary, we have presented a finite-size scaling study of the four-dimensional Edwards-Anderson model of an Ising spin glass in an external magnetic field. We have been able to reach large system sizes and low temperatures, thanks to the Janus special-purpose computer. Our finite-size scaling method avoids the anomalies observed in ref. 25. We present conclusive evidence for the presence of a de Almeida-Thouless line in the temperature-magnetic field phase plane (inset for Fig. 1), whose universality class we characterize. In other words, a spin-glass transition occurs, even without time-reversal symmetry, for realistic models (i.e., well below the upper critical dimension $d_u = 6$). A far-reaching consequence is that the universality class for the phase transition in structural glasses may actually exist (24). Our result also settles a longstanding controversy in the field of spin glasses (see, e.g., refs. 13, 14).

Materials and Methods

Simulations. We have carried out parallel tempering (38, 39) simulations for three values of the magnetic field (see Table S1 for details), with periodic boundary conditions. For each value of h, we have simulated 25,600 samples for $L \leq 12$ systems and between 1,000 and 4,000 in the $L = 16$ system.

Our thermalization protocol is sample dependent (see ref. 32 for details). We first perform a number of iterations large enough to ensure thermalization in a large fraction of the samples (typically 90%). We study the autocorrelation of the temperature flow during the parallel tempering and extend the runs for the slower samples until a total length of 14 exponential

Table 1. Critical temperatures and exponents for our model from a joint fit of our data at h=0.15 and $h = 0.3$

Parameter	$h = 0.3$	$h = 0.15$	$h = 0.075$[*]
$T_c(h)$	0.906(40)[3][†]	1.229(30)[2]	1.50(7)
ν	1.46(7)[6]		-
η	−0.30(4)[1]		-

[*] The data for this field was only used for a consistency check.

[†] Errors in square brackets are due to the uncertainty in ω.

[†] The data for $h = 0.075$ presented very severe corrections, probably due to the proximity of the $h = 0$ critical point. Therefore, we only use the data for $L \geq 12$ in order to estimate $T_c(h = 0.075)$.

autocorrelation times is ensured. The final product is a set of thermalized and almost independent configurations. As an example, each $L = 16$ sample in $h = 0.15$ was simulated at least for 5×10^7 heat bath lattice sweeps at each of the $N_T = 32$ temperatures (we performed a parallel tempering update every 10 heat baths). However, the hardest sample required as many as 2.6×10^{10} heat bath sweeps.

The $L = 16$ lattices were simulated on the Janus computer with an update speed (for each of its 256 units) of 86 ps per spin flip with a heat bath scheme. The $L \leq 12$ lattices were simulated on Personal Computer (PC) clusters, with a C code that uses multispin coding (40) with 128-bit words (using the streaming extensions); the update speed in this case is 350 ps per spin flip using a Metropolis algorithm (on an Intel Core2 processor at 2.40 GHz). With multispin coding, the samples whose simulations have to be extended must be extracted from the original 128-sample bundles to construct new bundles that are then extended with the same code. Note finally that, because the PC spreads the spin flips over 128 samples, the simulation for each sample is faster on Janus by a factor approximately 500. This difference is significant when the equilibration time is large.

The Correlation Functions. The main quantities that we compute are the correlation functions. In the presence of a magnetic field, the expectation of each spin $S_{\mathbf{x}}$ is nonvanishing. Hence we may consider these two correlation functions:

$$G_1(\boldsymbol{r}) = \frac{1}{L^4}\sum_{\mathbf{x}} \overline{(\langle S_{\mathbf{x}} S_{\mathbf{x}+\mathbf{r}}\rangle - \langle S_{\mathbf{x}}\rangle\langle S_{\mathbf{x}+\mathbf{r}}\rangle)^2}, \qquad \textbf{[9]}$$

$$G_2(\boldsymbol{r}) = \frac{1}{L^4}\sum_{\mathbf{x}} \overline{(\langle S_{\mathbf{x}} S_{\mathbf{x}+\mathbf{r}}\rangle^2 - \langle S_{\mathbf{x}}\rangle^2\langle S_{\mathbf{x}+\mathbf{r}}\rangle^2)}\,. \qquad \textbf{[10]}$$

In the above, the $\langle\cdots\rangle$ stands for the thermal average in a single sample, while the disorder average is indicated by an overline. Note that the Fourier transform $\hat{G}_1(\boldsymbol{k} = 0)$ is the spin-glass susceptibility. We simulate four real replicas $\{S_{\mathbf{x}}^{(a)}\}$ (i.e., four systems with the same couplings evolving independently under the thermal noise) in order to obtain unbiased estimators of the correlation functions. In the main text G stands for either of the $G_{1,2}$. In the fits we have combined data from both whenever it was useful to obtain smaller statistical errors.

The correlation functions were computed off-line over stored configurations. We note that configurations at different Monte Carlo times can be combined as long as they belong to different replicas (41). This combination results in small Monte Carlo errors with a modest number of configurations, so the uncertainty on the final result is dominated by the sample-to-sample fluctuations. This step is rather time consuming, so we also use multispin coding to accomplish it.

In order to define the second-moment correlation length (42), we consider the following Ornstein-Zernike expansion for the propagator in Fourier space,

$$\frac{1}{\hat{G}(\boldsymbol{k})} = \frac{\xi^2}{\hat{G}(0)}\left[\frac{1}{\xi^2} + k^2 + a_4(k^2)^2 + \ldots\right], \qquad \textbf{[11]}$$

where $k^2 = 4\sum_\mu \sin^2(k_\mu/2)$. Then, the common second-moment correlation length ξ_2 is obtained by truncating the expansion at the k^2 term:

$$\xi_2 = \frac{1}{2\sin(\pi/L)}\left(\frac{\hat{G}(0)}{\hat{G}(\boldsymbol{k}_1)} - 1\right)^{1/2}. \qquad \textbf{[12]}$$

As we comment in the main text, this definition is not well behaved for our model, due to the anomalous behavior of the $\boldsymbol{k} = 0$ mode. Actually, there is a simple, yet unexpected explanation for this anomaly. The anomalous behavior arises whenever soft excitations (Goldstone bosons) are present in the low-temperature phase, while an external magnetic field splits excitations into longitudinal and transversal (43). Familiar examples of Goldstone bosons are magnons, or the phonons in an acoustical branch. What is most peculiar about spin glasses is that soft modes are present (44, 45), even if our variables are discrete.

ACKNOWLEDGMENTS. We thank Davide Rossetti for introducing us to the handling of the 128-bit registers. We acknowledge partial financial support from Ministerio de Ciencia e Innovación (MICINN), Spain, (contract nos. FIS2009-12648-C03, FIS2010-16587, TEC2010-19207), from Universidad Complutense de Madrid (UCM)-Banco de Santander (GR32/10-A/910383), from Junta de Extremadura, Spain (contract no. GR10158), and from Universidad de Extremadura (contract no. ACCVII-08). B.S. and D.Y. were supported by the Formación de Profesorado Universitario (FPU) program (Ministerio de Educación, Spain); R.A.B. and J.M.-G. were supported by the Formación de Personal Investigador (FPI) program (Diputación de Aragón, Spain); finally J.M.G.-N. was supported by the FPI program (Ministerio de Ciencia e Innovación, Spain).

1. Debenedetti PG (1997) *Metastable Liquids* (Princeton University Press, Princeton).
2. Debenedetti PG, Stillinger FH (2001) Supercooled liquids and the glass transition. *Nature* 410:259–267.
3. Cavagna A (2009) Supercooled liquids for pedestrians. *Phys Rep* 476:51–124.
4. Mydosh JA (1993) *Spin Glasses: an Experimental Introduction* (Taylor and Francis, London).
5. Hérisson D, Ocio M (2002) Fluctuation-dissipation ratio of a spin glass in the aging regime. *Phys Rev Lett* 88:257202.
6. Cruz A, et al. (2001) SUE: A special purpose computer for spin glass models. *Computer Physics Communications* 133:165–176.
7. Ogielski A (1985) Dynamics of three-dimensional Ising spin glasses in thermal equilibrium. *Phys Rev B* 32:7384–7398.
8. Belletti F, et al. (2008) Simulating spin systems on IANUS, an FPGA-based computer. *Computer Physics Communications* 178:208–216.
9. Belletti F, et al. (2008) Nonequilibrium spin-glass dynamics from picoseconds to one tenth of a second. *Phys Rev Lett* 101:157201.
10. Gunnarsson K, et al. (1991) Static scaling in a short-range Ising spin glass. *Phys Rev B* 43:8199–8203.
11. Ballesteros HG, et al. (2000) Critical behavior of the three-dimensional Ising spin glass. *Phys Rev B* 62:14237–14245.
12. Palassini M, Caracciolo S (1999) Universal finite-size scaling functions in the 3D Ising spin glass. *Phys Rev Lett* 82:5128–5131.
13. Bray AJ, Moore MA (2011) Disappearance of the de Almeida-Thouless line in six dimensions. *Phys Rev B* 83:224408.
14. Parisi G, Temesvári T (2011) Replica symmetry breaking in and around six dimensions. *Nucl Phys B* 858:293–316.
15. Bray AJ, Roberts SA (1980) Renormalization-group approach to the spin glass transition in finite magnetic fields. *J Phys C Solid State* 13:5405–5412.
16. de Almeida JRL, Thouless DJ (1978) Stability of the Sherrington-Kirkpatrick solution of a spin glass model. *J Phys A* 11:983–990.
17. Fisher DS, Sompolinsky H (1985) Scaling in spin-glasses. *Phys Rev Lett* 54:1063–1066.
18. Young AP, Katzgraber HG (2004) Absence of an Almeida-Thouless line in three-dimensional spin glasses. *Phys Rev Lett* 93:207203.
19. Jörg T, Katzgraber H, Krzakala F (2008) Behavior of Ising spin glasses in a magnetic field. *Phys Rev Lett* 100:197202.
20. Jönsson PE, Takayama H, Aruga Jatori H, Ito A (2005) Dynamical breakdown of the Ising spin-glass order under a magnetic field. *Phys Rev B* 71:180412.
21. Petit D, Fruchter L, Campbell I (1999) Ordering in a spin glass under applied magnetic field. *Phys Rev Lett* 83:5130–5133.
22. Petit D, Fruchter L, Campbell I (2002) Ordering in Heisenberg spin glasses. *Phys Rev Lett* 88:207206.
23. Tabata Y, et al. (2010) Existence of a phase transition under finite magnetic field in the long-range RKKY Ising spin glass $\mathrm{Dy}_x\mathrm{Y}_{1-x}\mathrm{Ru}_2\mathrm{Si}_2$. *J Phys Soc Japan* 79:123704.
24. Moore M, Drossel B (2002) *p*-spin model in finite dimensions and its relation to structural glasses. *Phys Rev Lett* 89:217202.
25. Leuzzi L, Parisi G, Ricci-Tersenghi F, Ruiz-Lorenzo JJ (2009) Ising spin-glass transition in a magnetic field outside the limit of validity of mean-field theory. *Phys Rev Lett* 103:267201.
26. Amit DJ, Martin-Mayor V (2005) *Field Theory, the Renormalization Group and Critical Phenomena* (World Scientific, Singapore), third edition.
27. Di Francesco P, Saleur H, Zuber JB (1987) Critical Ising correlation functions in the plane and on the torus. *Nucl Phys B* 290:527–581.
28. Di Francesco P, Saleur H, Zuber JB (1988) Correlation functions of the critical Ising model on a torus. *Europhys Lett* 5:95–100.
29. Ballesteros HG, Fernandez LA, Martin-Mayor V, Muñoz Sudupe A (1996) New universality class in three dimensions?: the antiferromagnetic RP^2 model. *Phys Lett B* 378:207–212.
30. Billoire A, et al. (2011) Finite-size scaling analysis of the distributions of pseudo-critical temperatures in spin glasses. *J Stat Mech* P10019.
31. Baños RA, et al. (2010) Static versus dynamic heterogeneities in the $D = 3$ Edwards-Anderson-Ising spin glass. *Phys Rev Lett* 105:177202.
32. Yllanes D (2011) *Rugged free-energy landscapes in disordered spin systems* (UCM, Madrid).
33. Jörg T, Katzgraber HG (2008) Universality and universal finite-size scaling functions in four-dimensional Ising spin glasses. *Phys Rev B* 77:214426.
34. Marinari E, Zuliani F (1999) Numerical simulations of the 4D Edwards-Anderson spin glass with binary couplings. *J Phys A* 32:7447–7462.
35. Fisher DS, Huse DA (1988) Equilibrium behavior of the spin-glass ordered phase. *Phys Rev B* 38:386–411.

36. Hartmann AK (1999) Calculation of ground states of four-dimensional ±*J* Ising spin glasses. *Phys Rev E* 60:5135–5138.
37. Hukushima K (1999) Domain-wall free energy of spin-glass models: Numerical method and boundary conditions. *Phys Rev E* 60:3606–3613.
38. Hukushima K, Nemoto K (1996) Exchange monte carlo method and application to spin glass simulations. *J Phys Soc Jpn* 65:1604–1608.
39. Marinari E (1998) *in Advances in Computer Simulation*, eds J Kerstész and I Kondor (Springer-Verlag, Berlin).
40. Newman MEJ, Barkema GT (1999) *Monte Carlo Methods in Statistical Physics* (Clarendon Press, Oxford).
41. Baños RA, et al. (2010) Nature of the spin-glass phase at experimental length scales. *J Stat Mech* P06026.
42. Cooper F, Freedman B, Preston D (1982) Solving $\phi^4_{1,2}$ field theory with Monte Carlo. *Nucl Phys B* 210:210–228.
43. Zinn-Justin J (2005) *Quantum Field Theory and Critical Phenomena* (Clarendon Press, Oxford), fourth edition.
44. Bray AJ, Moore MA (1987) *Heidelberg Colloquium on Glassy Dynamics*, eds JL van Hemmen and I Morgenstern (Springer, Berlin), Lecture Notes in Physics No. 275, pp 121–153.
45. de Dominicis C, Kondor I, Temesvári T (1998) *in Spin Glasses and Random Fields*, ed AP Young (World Scientific, Singapore).